Properties of the two-temperature corona model for active galactic nuclei and galactic black holes

Agnieszka Janiuk [a,1] Bożena Czerny [a,1]

[a] *N. Copernicus Astronomical Center, Bartycka 18, 00-716 Warsaw, Poland*

Abstract

We study in detail the properties of the accreting corona model for active galactic nuclei and galactic black holes. In this model the fraction of the energy liberated in the corona at a given radius is calculated from the global parameters of the model (mass of the central object, accretion rate and viscosity parameter) and it appears to be a strong function of the radius. The model predicts the relative decrease of the coronal hard X-ray emission with an increase of the accretion rate. The presented description of disc/corona interaction forms a basis for further studies of disc disruption mechanism.

Key words: accretion, accretion discs – black hole physics – galaxies: active – X-rays: galaxies – X-rays: stars

1 Introduction

The accretion flow onto black holes both at the centers of active galactic nuclei (AGN) and galactic black holes (GBH) consists of two phases: relatively cold optically thick accretion disc responsible for multicolor black body emission and a hot optically thin plasma responsible for a power law shape X-ray emission.

There are two basic families of models of this two phase flow.

The first family assumes the radial division of the flow into hot and cold part, with outer part cold and the inner part hot and optically thin. That

[1] Partially supported by the Polish State Committee for Scientific Research, grant 2P03D018.16

line of research originated with the classical paper of Shapiro, Lightman and Eardley (1976) followed by a number of papers which differed with respect to the description of the heating and cooling mechanisms of the hot part and the position of the radius dividing the hot from the cold flow (e.g. Wandel & Liang 1991, Narayan, Kato & Honma 1997). Also a possibility of having an outer part hot and an inner part cold have been recently discussed (Dullemond & Turolla 1998).

The second family assumes the vertical division of the flow into hot and cold part, i.e. describes an accretion disc with a hot corona. First papers on this subject (e.g. Liang & Price 1977, Bisnovatyi-Kogan & Blinnikov 1977) were further followed by a number of papers adopting different descriptions of the fraction of energy liberated in the corona, heating and cooling of the corona and the disc/corona interaction (e.g. Haardt & Maraschi 1991, Svensson & Zdziarski 1994, Życki, Collin-Souffrin & Czerny 1995).

Some phenomenological models actually filled this gap assuming that there can be some overlapping between these two distinct possibilities, i.e. the innermost part of the flow is hot and optically thin, an intermediate part consists of a disc but covered by the hot plasma extending beyond the central region and the outermost part is a bare accretion disc (e.g. Poutanen, Krolik & Ryde 1997, Esin, McClintock & Narayan 1997, Magdziarz & Blaes 1997). However, such an intermediate region did not result from physically based assumptions but was introduced as a kind of ad hoc parameterization.

Both families of models have their advantages and disadvantages from the observational point of view.

Models of a single compact hot plasma cloud surrounding the central black hole are claimed to reproduce well the 'primary' X-ray spectrum for Cyg X-1 (e.g. Dove, Wilms & Begelman 1997) although other authors found some overlapping between the hot cloud and cold disc necessary (Poutanen et al. 1997) and perhaps stratification in the hot plasma temperature is required (Ling et al. 1997, Gierliński et al. 1997). However, these models predict too compact X-ray emitting region in order to explain within a frame of pure Comptonization model (Kazanas, Hua & Titarchuk 1997) long time/phase delays measured for that source (Cui et al. 1997). In the case of AGN, their X-ray spectra are also well modeled by comptonization in a single compact plasma cloud (e.g. Johnson et al. 1997 for NGC 4151, Gondek et al. 1996 for composite Seyfert spectrum) and a reflection from the cold gas.

Corona models are equally successful in modeling the data if certain arbitrary clumpiness of the corona is allowed (Haardt, Maraschi & Ghisellini 1994; see also Gondek et al. 1996). Models assuming continuous corona over-produce the ratio of the hard X-ray emission to the optical/UV/soft X-ray component

if the spectrum is flat and the same ratio of the dissipation in the disc and in the corona is adopted at all disc radii.

Both families of models usually contain a number of arbitrary parameters so they can give satisfactory fits to the observational data. This success makes the differentiation between the two geometrical models rather difficult. Further progress can be made using two approaches: either to look for a second order differences which may show up in high quality spectra or to make a step back and incorporate into the model only well justified ingredients.

This second, complementary approach is also valuable although it does not provide immediately as precise description of the observational data as the phenomenological one. If we only allow for a well known or reasonably parameterized *physical* input into the model we are on a track to prove or falsify the model. This approach requires first to study the properties of the resulting model and its sensitivity to the principal ingredients. The next step is to study in detail the discrepancies between the model predictions and the data in order to see whether those discrepancies can be accommodated within the frame of the model or not. This approach does not lead to the success (in the sense of reproducing data) immediately but the ultimate goal of understanding the underlying physics of accretion makes it worth to pursue.

A lot of work along such line is being done recently for advection-dominated accretion flow (ADAF) solutions (e.g. Quataert & Narayan 1998, Kato & Nakamura 1998, Gammie & Popham 1998, Di Matteo et al. 1998).

In this paper we adopt the same approach but to a two-temperature corona model based on two assumptions: (1) the dissipation in the corona is proportional to the pressure (2) vertical transition between the disk and the corona at each radius is determined by the marginal thermal stability of the Compton/atomic cooled medium. Such a model does not require any arbitrary parameterization of the transition between the hot and the cold plasma but nevertheless reproduces a broad range of the ratios between the bolometric luminosity of the optically thick disc and hot plasma emission. We show that this property results from strong radial dependence of the relative strength of the corona which is the intrinsic property of the model.

The properties of the corona (i.e. the electron and ion temperature, the optical depth and the fraction of total energy dissipated at a given radius measured in Schwarzschild radii) only weakly depend on the central mass of the black hole if the accretion rate is measured in Eddington units. Therefore, the same model applies without any major change to an AGN or a GBH. However, the radiation spectra given by the model are significantly influenced by the central mass due to the dependence of the disc temperature on its value.

The approach used is much simpler than that of Życki et al. (1995) and Witt

et al. (1997). Instead, the attention is payed to the prediction of the radial distribution of the disk/corona properties, the spectra and the sensitivity of the model to the description of the physical processes involved.

The contents of the paper is as following. In Section 2.1 we summarize the underlying assumptions which lead to much simpler description than the full dynamical treatment of Witt et al. (1997). In Section 2.2 we describe the computation method of the spectra integrated over the disk surface. Section 3.1 is devoted to analysis of the radial properties of the simplest corona model and its predicted extension. In Sections 3.2, 3.3, and 3.4 we analyze the importance of the accuracy of description of the X-ray transfer and ion-electron interaction. The results are discussed in Section 4 and conclusions given in Section 5.

2 Model

2.1 Disc/corona structure

In this model of accretion flow onto a black hole we assume that the (stationary) accretion is ultimately responsible for the emission of the radiation and therefore the accretion rate, $\dot{M}$, together with the mass of the central black hole, M, are the basic parameters of our model. The accretion proceeds predominantly through the disk which is surrounded, wherever possible, by a hot optically thin corona.

We assume that the hot optically thin corona is a two-temperature medium, as in the paper of Shapiro, Lightman & Eardley (1976), i.e. the ion temperature is higher than the electron temperature, the loss of gravitational energy by accreting gas is transported directly to the ions, Coulomb coupling transfers this energy to electrons and finally electrons cool down by Inverse Compton process, with disc emission acting as a source of soft radiation flux.

We approximate the distribution of the angular momentum in the disk and the corona by the Keplerian distribution so the sum of the flux generated by the disk, F_d, and by the corona, F_c, at any given radius is determined by the standard formula (see e.g. Kato, Fukue & Mineshige 1998)

$$F_d + F_c = \frac{3GM\dot{M}}{8\pi r^3} f(r), \tag{1}$$

where $f(r)$ represents the Newtonian boundary condition at the marginally

stable orbit

$$f(r) = 1 - (3R_{\rm Schw}/r)^{1/2}. \tag{2}$$

We describe the local heating of the ions in terms of the α viscosity introduced by Shakura & Sunyaev (1973) and we neglect the coronal radiation pressure since it should not contribute to energy generation in optically thin medium:

$$F_c = \frac{3}{2}\Omega_K \alpha P_o H \sqrt{\frac{\pi}{2}} \tag{3}$$

where P_o is the pressure at the basis of the corona, H is the pressure scale height of the corona given by the ion temperature, T_i, under the assumption of the hydrostatic equilibrium

$$H = \frac{1}{\Omega_K}\sqrt{\frac{kT_i}{m_H}} \tag{4}$$

and the factor $\sqrt{\pi}/2$ results from the vertical integration of the pressure (Witt, Czerny & Życki 1997, hereafter WCZ, Appendix D).

Such a formulation is independent from the physical mechanism of the corona heating since the scaling with pressure may correspond either to accreting corona which is powered directly by the release of the fraction of the gravitational energy of the accreting gas within the corona itself (e.g. Życki, Collin-Souffrin & Czerny 1995, WCZ) or to the magnetic heating (e.g. Svensson & Zdziarski 1994).

The net flux, $F_c + F_{nl}$, is subsequently transported to electrons through the electron-ion Coulomb interaction, as described by the following equation (Shapiro, Lightman & Eardley 1976)

$$F_c + F_{nl} = \frac{3}{2}\frac{k(T_i - T_e)}{m_H}\left[1 + \left(\frac{4kT_e}{m_e c^2}\right)^{1/2}\right]\nu_{ei}\rho_o H\frac{\sqrt{\pi}}{2}, \tag{5}$$

where T_e is the electron temperature, and

$$\nu_{ei} = 2.44 \times 10^{21}\rho_o T_e^{-1.5}\,\ln\Lambda \quad [s^{-1}]; \quad \text{with} \quad \ln\Lambda \approx 20 \tag{6}$$

is the electron-ion coupling rate. Here the density ρ_o is related to the corona thickness and its optical depth τ_{es}

$$\tau_{es} = k_{es}\rho_o H. \tag{7}$$

We discuss the accuracy of this description and the dependence of the model on the ion-electron coupling rate in Section 3.4.

The corona is assumed to be isothermal and its vertical density profile is taken into account only through the numerical factors in Eqs. (3) and (5).

The energy flux transferred to electrons has to be carried away by soft X-ray photons scattered by the corona

$$F_c + F_{nl} = A(\tau_{es}, T_e, T_s) F_{soft} \tag{8}$$

which constitute hard X-ray coronal emission. We discuss the results for two descriptions of the Compton amplification factor A. In Section 3.1 we present the results obtained using a simple analytic description of this factor by the Compton parameter y as in WCZ)

$$A(\tau_{es}, T_e, T_s) = e^y - 1; y = \tau_{es} \frac{4kT_e}{m_e c^2} \left(1 + \frac{4kT_e}{m_e c^2}\right) \tag{8a}$$

since is shows the properties of the model used by Czerny, Witt & Życki (1997) and Kuraszkiewicz, Loska & Czerny (1997) to compare to the AGN data. This method is very approximate but simple and convenient since it is independent on the soft photon energy and in that case the corona model is independent on the mass of the central black hole and can easily give results appropriate for a qualitative discussion (see WCZ, in particular Appendix C). In Section 3.2 we compare those results with the results based on the Monte Carlo simulations of the Comptonization process. The Monte Carlo code employs the method described by Pozdnyakov, Sobol & Sunyaev (1983) and Gòrecki & Wilczewski (1984). Assuming slab geometry (Thomson optical depth τ_{es} and electron temperature T_e) and the soft photons spectrum as a black body of temperature T_s determined by F_{soft}, we compute the amplification factor A on a grid of $T_e,\ \tau_{es},\ \text{and}\, T_s$. We compute A at each radius by interpolation. This method is more accurate than the use of the Compton parameter y. It introduces the dependence of the model on the mass of the central black hole (through T_s) and allows for more quantitative discussion.

The soft flux from the formula (8) is determined by the radiative coupling between the disc and the corona, as described in the basic paper of Haardt and Maraschi (1991). It means that the soft flux emitted by the disk consists of the sum of the flux generated by the disk interior and the fraction of the coronal radiation absorbed by the disk

$$F_{soft} = F_d + \eta(F_c + F_{nl})(1 - a) \tag{9}$$

In our basic model we assume that the fraction η of the coronal flux directed

towards the disk is equal 0.5 and the energy averaged albedo a is equal 0.2.

Our system of equations determining the corona structure, including the fraction of the energy, f, liberated in the corona ($f = F_c/(F_c + F_d)$) is closed by the following considerations.

The vertical division of the medium into hot corona and cold accretion disc at every radius should not be arbitrary, as it is customary assumed. Indeed, such a division results naturally from the criterion of thermal instability in an irradiated medium studied by Krolik, McKee and Tarter (1981). The ionization stage of the medium is conveniently expressed through a ionization parameter Ξ defined as a ratio of the ionization radiation pressure to the gas pressure

$$\Xi = \frac{\eta(F_c + F_{nl})}{cP_o}. \tag{10}$$

The transition from cold to hot medium is characterized quantitatively by a specific value of the ionization parameter Ξ which scales with the electron temperature as

$$\Xi = 0.65(T_e/10^8\mathrm{K})^{-3/2} \tag{11}$$

(Begelman, McKee & Shields 1983; see also Życki et al. 1995). We discuss this scaling in Section 3.4.

The set of equations (1) - (11) allows to calculate the radial structure of the corona as a function of global model parameters, i.e. mass of the black hole, M, the accretion rate, $\dot{M}$, and the viscosity parameter α in the corona, if the nonlocal contribution F_{nl} is specified. We frequently use throughout the paper the dimensionless accretion rate $\dot{m}$ measured in the Eddington units.

$$\dot{M}_{Edd} = 3.52\frac{M}{10^8 M_\odot}[M_\odot/yr], \tag{12}$$

where M is the mass of the central black hole. The value of the mass does not influence strongly the radial dependence of the coronal temperatures and its optical depth but it scales with the absolute value of the corona luminosity. We assume a non-rotating black hole so the inner disc radius is located at $3R_{Schw}$ and critical accretion rate was defined using the pseudo-Newtonian efficiency of accretion equal to 1/16 and pure hydrogen opacity.

The computations of the disc structure are not required to complete the model. Therefore, for the purpose of this study, we do not have to specify whether the corona is actually an accreting corona transporting the mass and angular momentum in the same way as the disc does or it is coupled to the disc through

the magnetic field and the disc has to carry the entire angular momentum flux (as assumed e.g. by Svensson & Zdziarski 1994) whilst the energy generation is proportional to the coronal gas pressure. However, having the corona properties determined, we can also study the vertical structure of the disc with appropriate boundary conditions at the disc surface (Różańska, et al. 1999) and assumption about the angular momentum transport.

The presented model differs from the model studied by WCZ by being simpler and at the same time more general. This model does not contain any dynamical terms connected with the motion of the coronal gas and therefore allows both for a slow inflow or outflow of the corona. We also study in detail the importance of the exact description of the Compton amplification factor and discuss the problem of corona formation in the context of the radiation pressure instability within a standard disc.

2.2 Spectra

We calculate the radiation spectrum emitted at each radius r separately.

Emission from the optically thick disc is computed neglecting the bound-free transitions but taking into account the effect of electron scattering (Czerny & Elvis 1987). The local density at the disc surface is determined by the hydrostatic equilibrium with the corona if corona develops at that radius, or it is taken to be equal to 0.1 of the mean disc density in the absence of the corona at that radius. This simplified method give similar results to the more advanced method developed for a disc without a corona by Dörrer et al. (1996).

Soft photons emitted locally by the disc are Comptonized by the corona if a corona develops at that radius. Its parameters: the optical depth $\tau_{es}(r)$ and the electron temperature $T_e(r)$ are computed from the model. The effect of Comptonization in our Model A is calculated as by Czerny & Zbyszewska (1991). In the case of Model B Monte Carlo simulations are performed, as described by Janiuk, Życki & Czerny (1999).

At present we do not include the spectral component which results from the reflection of the X-rays from the disc surface since we concentrate on the qualitative study of the model possibilities. Any future attempt to fit the model to the observational data will have to include this component as well.

The final disc spectrum is computed by integration over the disc surface assuming an inclination angle equal zero (i.e. top view). All computations are done for a non-rotating black hole and the relativistic corrections were neglected.

3 Results

3.1 Model A: simplified description of Comptonization

In this section we present the properties of the corona calculated without any nonlocal heating-cooling term, i.e. $F_{nl} = 0$ in Equations (1)-(11). We describe the efficiency of the Compton cooling using the analytic approximation (Eq. 8a). Such a corona is fully determined at each radius by just two parameters: the accretion rate $\dot{m}$ expressed in the Eddington units and the viscosity parameter α, if the radius is expressed in units of the Schwarschild radii. Such a scaling is natural if a disc temperature does not have to be considered and it was frequently used to reduce the number of free parameters in the description of a hot plasma (see e.g. Björnsson & Svensson 1992).

3.1.1 The relative strength of the corona

The most important property of the accreting corona model is the strong radial dependence of the strength of the corona.

An example of the radial dependence of the fraction of energy generated in the corona is shown in Figure 1. The local value f is defined (after Haardt & Maraschi 1991) as the fraction of energy dissipated in the corona. Note that WCZ used ξ - a fraction of energy liberated in the disc - but these two quantities are complementary (i.e. $f = 1 - \xi$).

Simplified analytical solutions to the corona structure show (see WCZ, Appendix C) that approximately this fraction of the energy f increases with the radius r as $f \propto r^{3/8}$. It means that the X-ray flux $F_X(r)$ actually decreases with radius since the total flux generated in the disc decreases as r^{-3} but this decrease is slower than the decrease of the total flux: $F_X(r) \propto r^{-3+3/8}$. This is important from the point of view of the spectral shape of the reflection component and the iron K_α line but, at present, we do not include the reflection component in the spectra.

The corona covers only the inner part of the disc starting from a certain radius r_{max}. At that radius all the energy is liberated in the corona (f=1). At larger radii no corona solutions of our equations exist. The Compton cooling provided by the disc is too large under the adopted assumptions about the corona structure. Any additional (constant) cooling decreases r_{max} whilst any additional (constant) heating increases it.

Therefore there is a strong and discontinuous change of accretion flow structure at that radius since for larger radii all the accretion proceeds thorough a disc

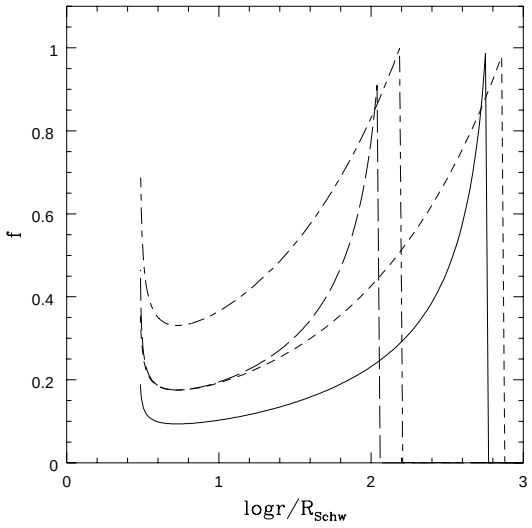

Fig. 1. Model A: The fraction of the energy dissipated in the corona as a function of radius for two values of the viscosity parameter α and two values of the accretion rate $\dot{m}$: $\dot{m} = 0.1$, $\alpha = 0.03$ (short dashed line), $\dot{m} = 0.1$, $\alpha = 0.33$ (continuous line), $\dot{m} = 0.01$, $\alpha = 0.03$ (short - long dashed) and $\dot{m} = 0.01$, $\alpha = 0.33$ (long dashed)

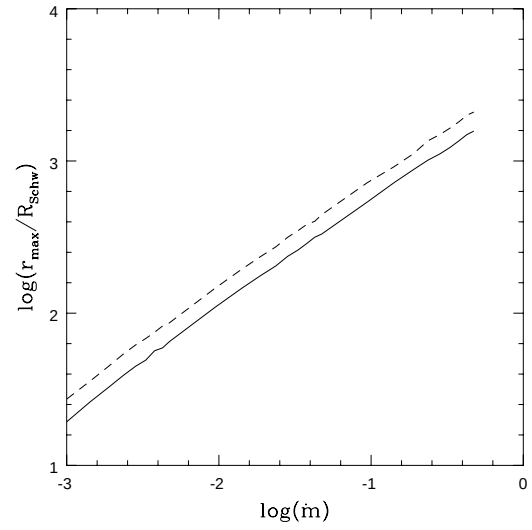

Fig. 2. Model A: The dependence of the extension of the corona on the accretion rate for the viscosity parameter α equal 0.03 (dashed line) and 0.33 (continuous line)

whilst suddenly, at r_{max}, rapid evaporation takes place, the dissipation of energy concentrates in the hot corona and the cold disc is heated up only by X-ray illumination. Closer in the relative strength of the corona decreases.

The dependence of the radial extension r_{max} of the corona on the accretion rate is shown in Figure 2. The size of the corona is considerable, covering the

disc up to $\sim 1000 R_{Schw}$ for large accretion rate but it decreases significantly for smaller accretion rates, down to about $100 R_{Schw}$ for sources radiating at 1% of the Eddington luminosity. The influence of the value of the viscosity parameter on the extension of the corona is rather weak.

3.1.2 Ion and electron temperatures and the optical depth

The ion temperature is a decreasing function of the radius (see Figure 3). It falls down almost linearly (see simplified formulae in Appendix C of WCZ).

In this paper we use simplified description of the vertical hydrostatic equilibrium and we have to check afterwards whether the solution can actually be in the hydrostatic equilibrium. The approximate criterion is that the ion temperature should be smaller than the local virial temperature. We see from Figure 3 that for low values of the viscosity parameter this requirement is not satisfied unless the accretion rate is smaller than about 1% of the Eddington value. In WCZ the vertical structure was calculated taking into account the transonic vertical outflow from the corona. In that case the solutions for small values of viscosity parameter and large accretion rates simply did not exist (see Figs. 1 and 3 of WCZ).

The pressure height scale of the corona defined as

$$H_P = (\frac{kT_i r^3}{GMm_H})^{1/2} \tag{13}$$

increases almost linearly with the radius (see Figure 4) and the H_P/r ratio is almost constant.

The formal solutions for high accretion rate and low viscosity which are characterized by the ion temperature being higher than the virial temperature show their problems in Figure 4 as well since in those cases the height of the corona at a given radius is larger than that radius. Therefore our model does not offer correct solution beyond certain range of parameters. If the model includes all the dynamical terms as in WCZ the physical problem of the character of the accretion flow is not solved since the solutions of the full set of differential equations (which require hydrostatic equilibrium at the basis of the corona) disappear when the ion temperature would exceed the virial temperature.

Since the density in the corona decreases outward the efficiency of Coulomb interaction between the ions and electrons decreases. However, both the disc and the corona bolometric luminosity go rapidly down with the radius. Therefore the electron temperature rises outwards and the ratio of the ion to electron temperature decreases outwards. The highest value of the electron tempera-

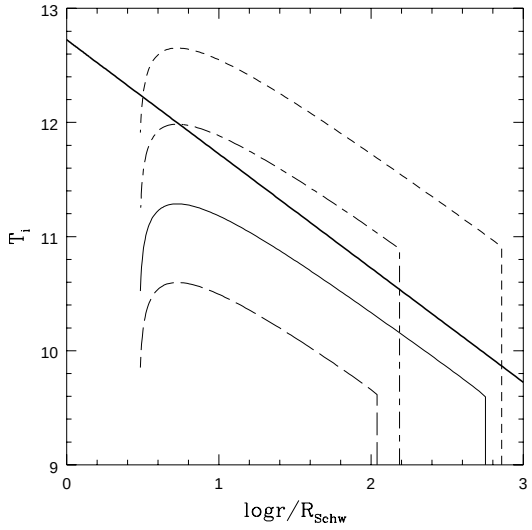

Fig. 3. Model A: The ion temperature as a function of radius for two values of the viscosity parameter α and two values of the accretion rate $\dot{m}$: $\dot{m} = 0.1$, $\alpha = 0.03$ (short dashed line), $\dot{m} = 0.1$, $\alpha = 0.33$ (continuous line), $\dot{m} = 0.01$, $\alpha = 0.03$ (short - long dashed) and $\dot{m} = 0.01$, $\alpha = 0.33$ (long dashed). The thick straight line shows the distribution of the local virial temperature.

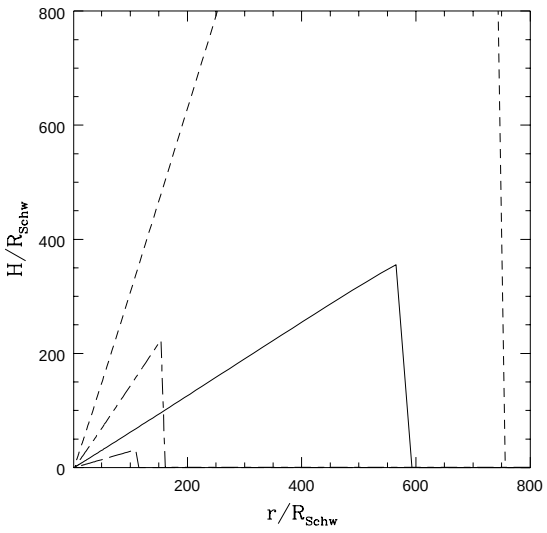

Fig. 4. Model A: The approximate shape of the corona given as a pressure height scale for two values of the viscosity parameter α and two values of the accretion rate $\dot{m}$: $\dot{m} = 0.1$, $\alpha = 0.03$ (short dashed line), $\dot{m} = 0.01$, $\alpha = 0.33$ (continuous line), $\dot{m} = 0.01$, $\alpha = 0.03$ (short - long dashed) and $\dot{m} = 0.01$, $\alpha = 0.33$ (long dashed)

ture is reached at r_{max}. Its value is roughly of the order of 3×10^9 K, independently from the accretion rate and the viscosity α. The precise value varies from 1.5×10^9 K for α equal 0.33 to 4.2×10^9 K for $\alpha = 0.03$ and its dependence on accretion rate is negligible. Such a universal value is an interesting

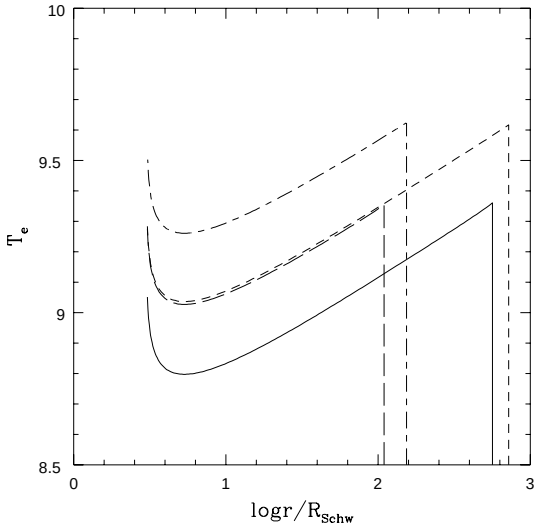

Fig. 5. Model A: The electron temperature as a function of radius for two values of the viscosity parameter α and two values of the accretion rate $\dot{m}$: $\dot{m} = 0.1$, $\alpha = 0.03$ (short dashed line), $\dot{m} = 0.1$, $\alpha = 0.33$ (continuous line), $\dot{m} = 0.01$, $\alpha = 0.03$ (short - long dashed) and $\dot{m} = 0.01$, $\alpha = 0.33$ (long dashed)

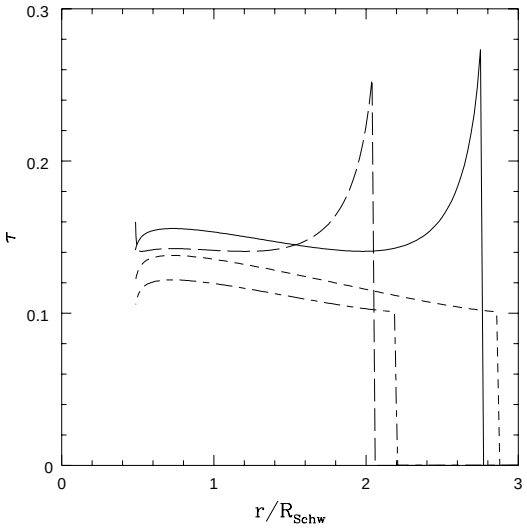

Fig. 6. Model A: The optical depth as a function of radius for two values of the viscosity parameter α and two values of the accretion rate $\dot{m}$: $\dot{m} = 0.1$, $\alpha = 0.03$ (short dashed line), $\dot{m} = 0.1$, $\alpha = 0.33$ (continuous line), $\dot{m} = 0.01$, $\alpha = 0.03$ (short - long dashed) and $\dot{m} = 0.01$, $\alpha = 0.33$ (long dashed)

property of our model and it is directly related to the predicted properties of the spectra.

3.1.3 Radiation spectra for AGN

Standard optically thick accretion disc models for parameters adequate for AGN predict that most emission concentrates in UV/soft X-ray band forming a Big Blue Bump spectral component. In our model this basic property is preserved but a fraction of the total bolometric luminosity is emitted also in hard X-rays due to the Compton cooling of the corona.

The fraction of the bolometric luminosity emitted in the form of hard X-rays decreases with increasing accretion rate. It also strongly depends on the adopted viscosity parameter, as seen from Figure 7. Larger viscosity leads to more profound Big Blue Bump since the radial extension of the corona is larger in that case and the generation of hard X-rays is systematically shifted towards larger disc radii where the gravitational energy available is lower.

Hard X-ray band above 20 keV is dominated by the emission of the outermost part of the corona. Since the temperature there is high and almost universal the spectrum is always practically flat on νF_ν diagram and its extension is only weakly dependent on the viscosity parameter and almost independent on the accretion rate.

In the soft X-ray band the spectrum shows more curvature than the simple models composed from a standard accretion disc without a corona and a single power law since the X-ray emission generated at inner radii provide an additional steeper component since the corona temperature there is lower than in the outer parts.

Generally, the spectra for massive black holes are easy to parameterize since the contribution from the disc and the corona form quite well separated components. From the observational point of view they can be well represented giving the α_{ox} index (which expresses directly the dominance of the Big Blue Bump) and the slope of the hard X-ray part, α_x.

The distribution of the α_{ox} was studied by Czerny et al. (1997). It compares favorably with the observed distribution for quasars and Seyfert galaxies although there are a few objects with properties beyond the range expected from the model.

The dependence of α_x on the accretion rate and the viscosity parameter α is shown in Figure 8.

We see that there is a weak trend in the change of the hard X-ray slope with the accretion rate. In the case of low viscosity the spectra are systematically harder for lower luminosity to the Eddington luminosity ratio. For high viscosity, this dependence is not monotonic.

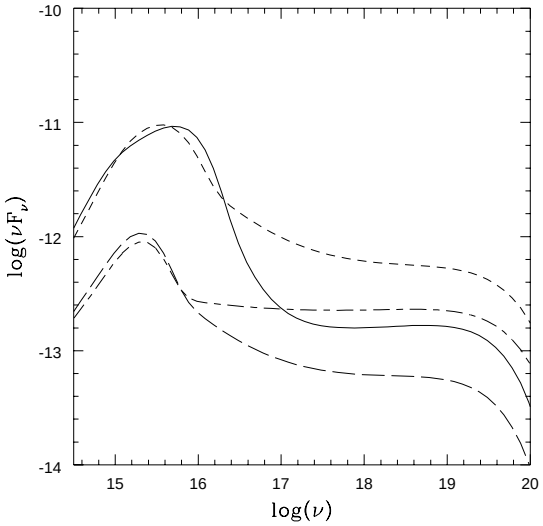

Fig. 7. Model A: The radiation spectrum for $M = 10^8 M_\odot$ and for two values of the viscosity parameter α and two values of the accretion rate $\dot{m}$: $\dot{m} = 0.1$, $\alpha = 0.03$ (short dashed line), $\dot{m} = 0.1$, $\alpha = 0.33$ (continuous line), $\dot{m} = 0.01$, $\alpha = 0.03$ (short - long dashed) and $\dot{m} = 0.01$, $\alpha = 0.33$ (long dashed)

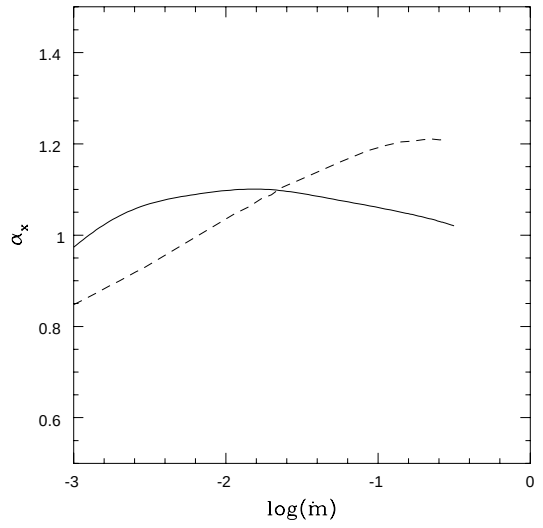

Fig. 8. Model A: The dependence of the 2-10 keV energy index α_x on the accretion rate for $M = 10^8 M_\odot$ and the viscosity parameter α equal 0.03 (dashed line) and 0.33 (continuous line)

3.1.4 Radiation spectra for GBH

As in the standard accretion disc models, low value of the mass of the central black hole results in much higher disc temperature and the optically thick component peaks in the soft X-ray band. This fact affects the spectral shape even in hard X-rays although the physical parameters of the corona model

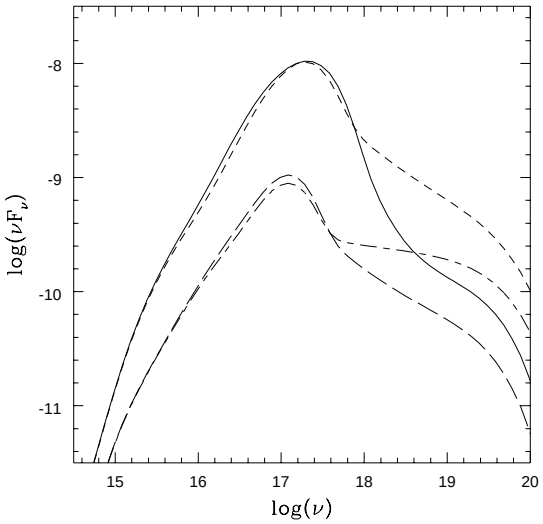

Fig. 9. Model A: The radiation spectrum for $M = 10M_{\odot}$ and for two values of the viscosity parameter α and two values of the accretion rate $\dot{m}$: $\dot{m} = 0.1$, $\alpha = 0.03$ (short dashed line), $\dot{m} = 0.1$, $\alpha = 0.33$ (continuous line), $\dot{m} = 0.01$, $\alpha = 0.03$ (short - long dashed) and $\dot{m} = 0.01$, $\alpha = 0.33$ (long dashed)

like the electron temperature and the optical depth are independent on the mass of the central black hole. Since the hard X-ray emission is caused by Comptonization of the optically thick disc emission higher disc temperature changes the slope of the hard X-rays leading to spectra being systematically steeper (softer) than in the case of AGN.

Since in GBH the difference between the disc and the corona electron temperature is smaller the hard power law part of the spectrum is also shorter and the spectral components are not as distinctive as in AGN. Nevertheless, in order to show quantitatively the basic trends we plot in Figure 10 the dependence of the hard X-ray spectral index on the accretion rate and the viscosity parameter.

The extension of the spectrum predicted by the model is the same as for AGN since it is determined by the maximum value of the electron temperature achieved in the corona (see Figure 5).

3.2 Model B: Monte Carlo description of Compton cooling and radiation spectra

Here we present the corona structure determined from the accurate description of the Compton cooling based on the Monte Carlo computations of the amplification factor A in Equation (8).

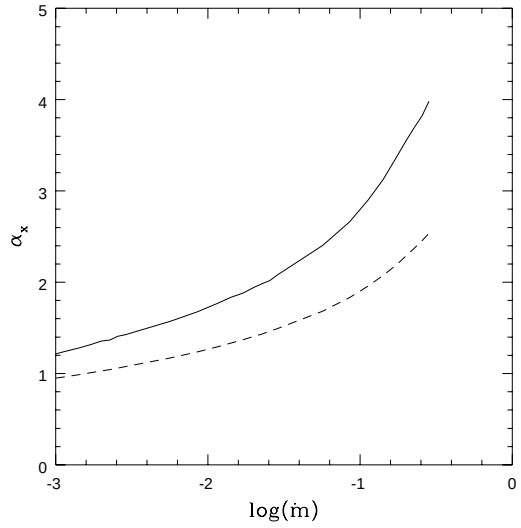

Fig. 10. Model A: The dependence of the 10-30 keV energy index α_x on the accretion rate for $M = 10M_\odot$ and the viscosity parameter α equal 0.03 (dashed line) and 0.33 (continuous line)

In this case the amplification factor depends on the soft photon energy, i.e. the temperature distribution along the accretion disc surface. The results of the corona structure have to be presented separately for the large masses appropriate for AGN and small masses typical for the GBH.

Qualitatively, the radial dependencies of the corona parameters are the same as presented in Section 3.1. The fraction of the disc covered by the corona is constrained to radii smaller than the critical value, r_{max} and the corona strength increases with radius for a given accretion rate till r_{max} where all the energy is dissipated within a corona.

However, there are clear systematic differences between the profiles presented in the previous Section and below.

In the case of the central black hole of $10M_\odot$ the change is the least important for high accretion rate and high viscosity. For low viscosity and low accretion rate the change is most profound. The radial extension of the corona is reduced considerably. The electron temperature is lower by a factor of 2. The optical depth is also slightly lower, particularly at the outer edge of the corona. It reflects the fact that the numerical value of the amplification factor is generally slightly higher than predicted by the Eq. (8a).

More accurate description of the Compton cooling did not help to solve the problem of the too high ion temperature in the model. Actually, the new results (compare Figure 3 and Figure 12) still enhanced the major problem of the corona not being in hydrostatic equilibrium by giving still higher values

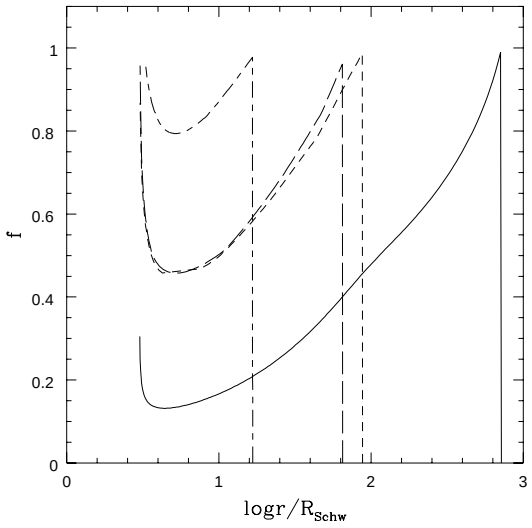

Fig. 11. Model B: The fraction of the energy dissipated in the corona as a function of radius for two values of the viscosity parameter α and two values of the accretion rate $\dot{m}$: $\dot{m} = 0.1$, $\alpha = 0.03$ (short dashed line), $\dot{m} = 0.1$, $\alpha = 0.33$ (continuous line), $\dot{m} = 0.01$, $\alpha = 0.03$ (short - long dashed) and $\dot{m} = 0.01$, $\alpha = 0.33$ (long dashed). Mass of the black hole $M = 10M_{\odot}$.

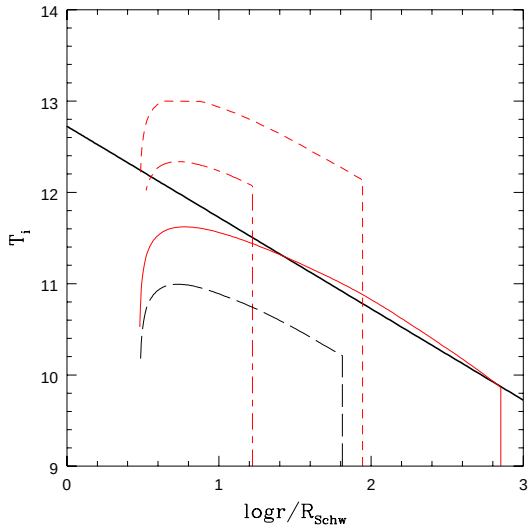

Fig. 12. Model B: The ion temperature as a function of radius for two values of the viscosity parameter α and two values of the accretion rate $\dot{m}$: $\dot{m} = 0.1$, $\alpha = 0.03$ (short dashed line), $\dot{m} = 0.1$, $\alpha = 0.33$ (continuous line), $\dot{m} = 0.01$, $\alpha = 0.03$ (short - long dashed) and $\dot{m} = 0.01$, $\alpha = 0.33$ (long dashed). The thick straight line shows the distribution of the local virial temperature. Black hole mass $M = 10M_{\odot}$.

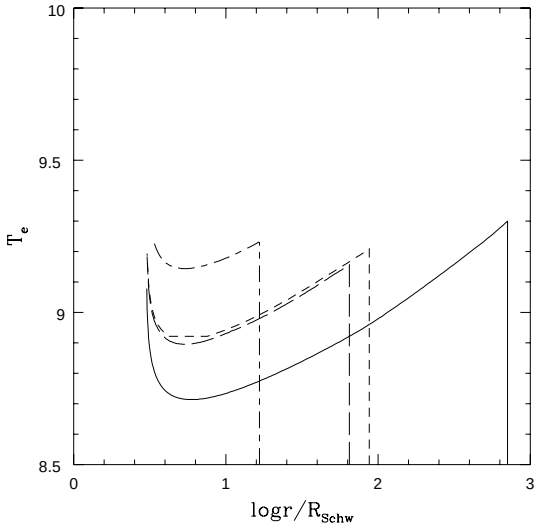

Fig. 13. Model B: The electron temperature as a function of radius for two values of the viscosity parameter α and two values of the accretion rate $\dot{m}$: $\dot{m} = 0.1$, $\alpha = 0.03$ (short dashed line), $\dot{m} = 0.1$, $\alpha = 0.33$ (continuous line), $\dot{m} = 0.01$, $\alpha = 0.03$ (short - long dashed) and $\dot{m} = 0.01$, $\alpha = 0.33$ (long dashed). Black hole mass $M = 10M_{\odot}$.

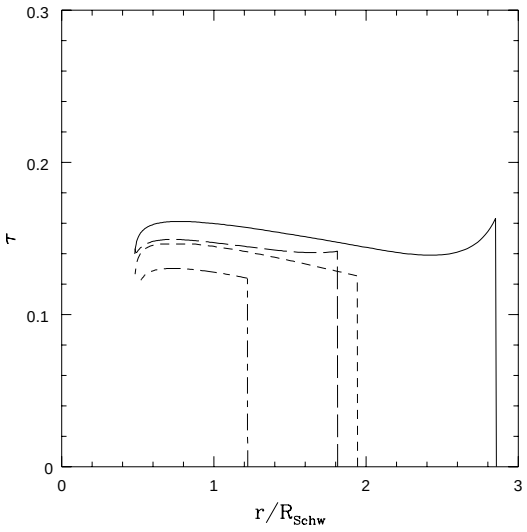

Fig. 14. Model B: The optical depth as a function of radius for two values of the viscosity parameter α and two values of the accretion rate $\dot{m}$: $\dot{m} = 0.1$, $\alpha = 0.03$ (short dashed line), $\dot{m} = 0.1$, $\alpha = 0.33$ (continuous line), $\dot{m} = 0.01$, $\alpha = 0.03$ (short - long dashed) and $\dot{m} = 0.01$, $\alpha = 0.33$ (long dashed). Mass of the black hole $M = 10M_{\odot}$.

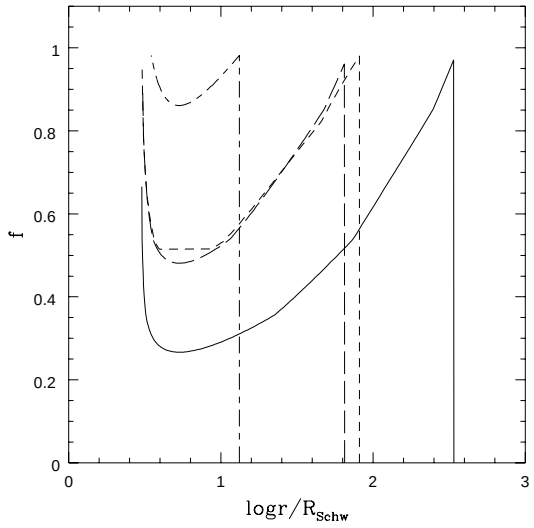

Fig. 15. Model B: The fraction of the energy dissipated in the corona as a function of radius for two values of the viscosity parameter α and two values of the accretion rate $\dot{m}$: $\dot{m} = 0.1$, $\alpha = 0.03$ (short dashed line), $\dot{m} = 0.1$, $\alpha = 0.33$ (continuous line), $\dot{m} = 0.01$, $\alpha = 0.03$ (short - long dashed) and $\dot{m} = 0.01$, $\alpha = 0.33$ (long dashed). Mass of the black hole $M = 10^8 M_\odot$.

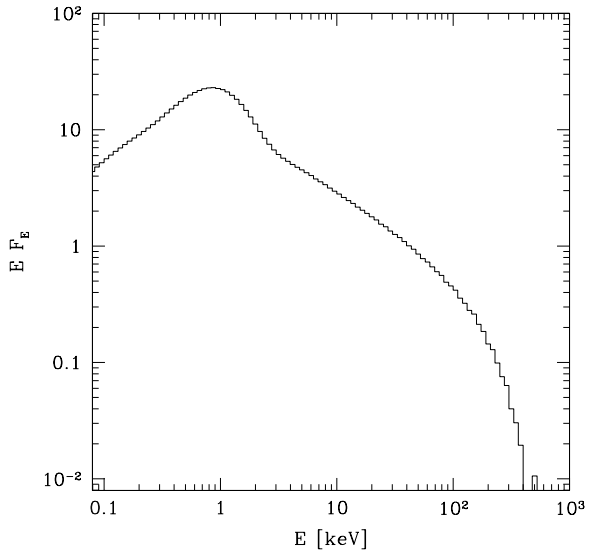

Fig. 16. Model B: The radiation spectrum for of the viscosity parameter $\alpha = 0.33$ and the accretion rate $\dot{m} = 0.01$, Mass of the black hole $M = 10 M_\odot$.

of the ion temperature for all presented cases of viscosity and accretion rate.

The results for AGN (i.e. assuming the mass of the black hole $10^8 M_\odot$) are similar and the change from the simpler solutions presented in Section 3.1 even larger. Corona shrinked also for the large accretion rate and large viscosity and the ion temperature is equally high.

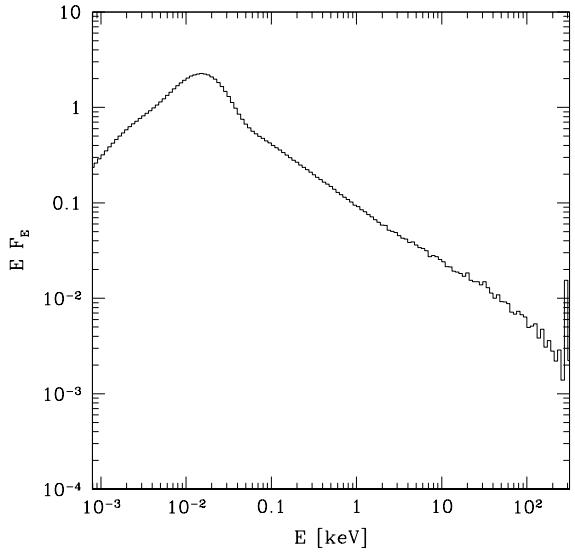

Fig. 17. Model B: The radiation spectrum for of the viscosity parameter $\alpha = 0.33$ and the accretion rate $\dot{m} = 0.01$, Mass of the black hole $M = 10^8 M_\odot$.

In Figures 16 and 17 we present the radiation spectra calculated using the Monte Carlo description of Compton cooling. The spectral slope in case of the black hole mass equal to $10M_\odot$ is almost the same as in the case of simplified description of Comptonization (Fig. 9), however in case of $10^8 M_\odot$ the spectrum is much softer (Fig. 7).

3.3 The effect of nonlocal radiative cooling

Since most of the energy is released close to the black hole the radiation flux illuminating the outer parts of the disc may dominate the radiation flux locally released due to accretion. This well known phenomenon (see e.g. Frank, King & Raine 1995) may have its source in either scattering of the central radiation by the extended corona or in direct illumination by the central source. The latter is important when the irradiating source is located at a certain height above a flat disc or when the disc is flaring in its outermost, gas pressure dominated region and its surface is exposed to the central flux.

The disc flaring, considered in the case of AGN, is present at radii $r > 10^4 R_{Schw}$ and in our model needs not to be taken into account. As for the effect of both direct and scattered flux, such irradiation has been studied in some detail for Compton heated coronae (see e.g. Kurpiewski, Kuraszkiewicz & Czerny 1997, and the references therein). It is important only if the luminosity of an object is very close to the Eddington luminosity. The same is true for our model which can be seen from following considerations.

In the case of irradiation by the flux scattered in the corona we can simply estimate the irradiating soft flux F_{scat} as a function of radius from the formula:

$$F_{scat} \approx \frac{L\tau_{\perp}}{4\pi r^2}\exp(-\tau_{\parallel}); \qquad exp(-\tau_{\parallel}) \approx (r/r_o)^{\frac{-\tau_{\perp} r}{H_P}}, \tag{14}$$

where $\tau_{\perp}$ is the typical optical depth of the corona as measured perpendicularly to the disc surface and $\tau_{\parallel}$ is the optical depth of the corona integrated radially from the radius of maximum energy generation r_o up to the current radius r. The power law dependence results from the radial density profile of the corona.

The direct incident flux emitted by the source located at the height $H_P/2$ depends on the angle between the direction of radiation and disc normal: $F_{direct} = L/4\pi D^2 \cos\Theta$, where $D \approx r$. Therefore the irradiating flux can be described by the formula:

$$F_{direct} \approx \frac{L}{8\pi r^3}\frac{H_P}{2}\exp(-\tau_{\parallel}). \tag{15}$$

As the locally generated soft flux depends on radius as r^{-3} the ratio of the directly irradiating to the locally emitted flux depends on radius only via $\tau_{\parallel}$:

$$\frac{F_{direct}}{F_{local}} \approx \frac{1}{12}\frac{H_P}{r_{ms}}\exp(-\tau_{\parallel}(r)), \tag{16}$$

where H_P is the height at $10R_{Schw}$, where most of energy dissipation takes place, and r_{ms} denotes the radius of marginally stable orbit.

We computed few examples of the model taking into account an increase of the soft radiation flux of the disc by the illumination as described above. The resulting electron temperature profile was hardly changed for lower accretion rate because of small geometrical extension of the corona and considerable radial optical depth. The effect somewhat increased for larger values of accretion rate: for $\dot{m} = 0.1$ the temperature of the outermost part of the corona lowered as a result by 20%, without a noticeable change in the inner parts. The conclusion that, within the frame of our model, the electron temperature reaches its highest value at the outer edge of the corona is not likely to be changed if the detailed, two-dimensional radiative transfer is solved for the corona.

3.4 Model dependence on Coulomb coupling and ionization parameter

The Compton amplification factor discussed in the previous Section is one of the physical ingredients built into the model. Two others are: the Coulomb coupling between the ions and electrons and the ionization parameter at the boundary between the disc and the corona.

WCZ used the Coulomb coupling rate after Shapiro et al. (1976; see Spitzer 1962) and assumed $ln\Lambda = 20$. Results presented in Sections 3.1 and 3.2 followed this approach. This description corresponds to the pure hydrogen plasma and it is correct only in the limit of $T_i/m_H \leq T_e/m_e$. The need for more accurate description was stressed recently by Zdziarski (1998).

We therefore replace the Equation (6) with the equation

$$\frac{dE}{dt} = -\frac{3m_e}{2m_p} N_e N_p \sigma_T c \times \frac{(kT_e - kT_p)}{K_2(1/\Theta_e)K_2(1/\Theta_p)} \ln\Lambda \times \left[\frac{2(\Theta_e+\Theta_p)^2+1}{\Theta_e+\Theta_p} K_1\left(\frac{\Theta_e+\Theta_p}{\Theta_e\Theta_p}\right) + 2K_0\left(\frac{\Theta_e+\Theta_p}{\Theta_e\Theta_p}\right)\right] \quad (17)$$

after Stepney & Guilbert (1983) and Zdziarski (1998), where $\Theta_e = kT_e/m_e c^2$ and $\Theta_p = kT_p/m_p c^2$.

The net effect of this change is a decrease of the Coulomb coupling rate by a factor 2. The model calculated with the new Coulomb coupling rate for the viscosity $\alpha = 0.03$ does not allow for any coronal solutions. Larger viscosity model ($\alpha = 0.3$) gives very similar solutions to these obtained using Shapiro et al. description of cooling, provided the accretion rate is small ($\dot{m} = 0.01$). In the case of higher accretion rates ($\dot{m} = 0.1$) the resulting optical depth of the corona is larger in its innermost parts and achieves value of 0.3. The corona covered region is slightly smaller in that case.

Since it was suggested (e.g. Begelman & Chiueh 1988, Bisnovatyi-Kogan & Lovelace 1997) that other more efficient mechanisms heating electrons might operate in a two-temperature plasma we also make a simple exercise by multiplying the original coupling rate from Equation (5) by a factor 2. This change leads to more extended corona. For low viscosity ($\alpha = 0.03$) the electron temperature increased up to $\sim 3\times10^9$K at the outer edge but the optical depth of the corona decreases down to ~ 0.05. The ion temperature was reduced by a factor ~ 3 but it was still higher than the virial temperature. Further increase of the coupling rate leads to unacceptably high electron temperature.

The model is therefore very sensitive to the microscopic description of the mechanism of energy transfer between ions and electrons.

The accuracy of the description of the boundary between the disc and the corona reflecting the change of cooling mechanism from Inverse Compton to atomic cooling is more difficult to discuss. The full description of the disc/corona transition is not available and only partial answers to this problem were considered so far. Maciołek-Niedźwiecki, Krolik & Zdziarski (1997) studied the role of the conductivity in the corona characterized by direct heating of electrons (no ion-electron coupling needed). Różańska & Czerny (1996) and Różańska (1999) considered the conductivity and both the Inverse Compton and atomic cooling but only in the case of radiatively heated one-temperature corona.

Therefore we make a simple exercise of a change in the scaling constant 0.65 in Eq. (11). An increase of this constant to 0.71 leads to an increase of the ion temperature thus engraving the problems with the hydrostatic equilibrium. It also causes a slight shrink of the region occupied by the corona. Further increase of this constant, to 0.85 causes a disappearance of the coronal solutions for low viscosity. A decrease of this constant to 0.55 leads to slight expansion of the corona covered region, a decrease of the ion temperature but it also decreases the optical depth of the corona.

3.5 Corona formation

The model, as outlined in Section 2, describes a two-temperature corona in thermal equilibrium but does not answer the question of the corona formation and stability.

Thermal stability of the two-temperature plasma described as in Shapiro, Lightman & Eardley (1976) has been studied by Pringle (1976). The model has been found to be unstable, i.e. small fluctuations of the ion temperature lead to the departure from the equilibrium. The same is true about the underlying disc when the corona is not strong enough to stabilize it (e.g. Czerny, Czerny & Grindlay 1986, Svenson & Zdziarski 1994). This may pose a problem to the model although, on the other hand, may be convenient if we recall the fact that all AGN and GBH are moderately or strongly variable so the stationary equations can at best provide an adequate description of some average state.

However, it also means that the presented set of equations does not describe the physical mechanism leading to corona formation. To answer this question we may look for instability mechanisms operating in the bare accretion disc which may lead spontaneously to thermal stratification and finally to the equilibrium state described by our model.

It is well known that $\alpha-$viscosity discs are unstable in their radiation pressure dominated parts (Pringle, Rees & Pacholczyk 1973, Shakura & Sunyaev 1976).

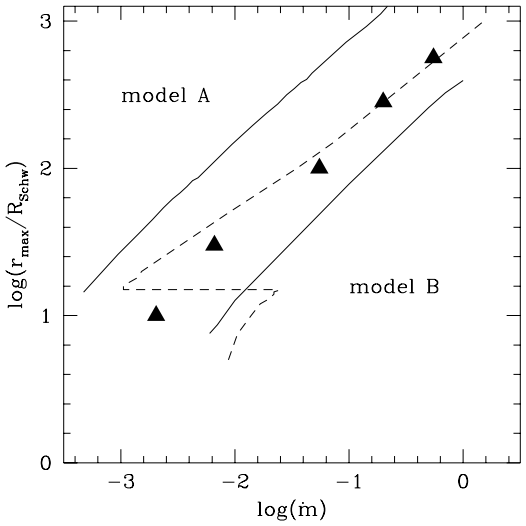

Fig. 18. The extension of the radiation pressure instability zone estimated from the vertically averaged disc model (dashed line) and from the model with the vertical structure included (triangles). The existence of inner stable ring for $\dot{m}$ between ~ 0.025 and 0.001 in vertically averaged models is caused by the opacity; this zone disappears in models with the vertical structure. Continuous lines show the extension of the corona covered zone given by Model A and Model B, correspondingly. Mass of the black hole is $M = 10^8 M\odot$ and the disc viscosity parameter is $\alpha_d = 0.03$.

However, if a presence of magnetic field is allowed within a disc, there is also photon bubble instability (Gammie 1998) which develops in the same region and seems to be characterized by even shorter timescale than the thermal instability. Any of those instabilities may in principle lead to corona formation and the detailed study of this process is beyond the scope of the present paper.

However, the attempt to identify the region of the corona development $r \leq r_{max}$, with the onset of the radiation pressure instability is tempting. Therefore in this section we study the radial extension of the disc instability zone and we discuss the possibility to adjust either the viscosity in the disc and in the corona or the nonlocal outflow in such a way as to make this two regions to coincide.

3.5.1 Radiation pressure instability

The criterion for the onset of the radiation pressure instability in a pure hydrogen disc was given by Shakura & Sunyaev (1976) ($\beta \leq 2/5$, where β is the gas pressure to the total pressure ratio), and the extension of the region approximately corresponding to this criterion ($\beta \leq 1/2$) was already estimated by Shakura & Sunyaev (1973).

The onset of instability, however, depends significantly on the description of opacities (e.g. Huré 1998). Applying the correct opacities to the vertically averaged disc structure leads to difficulties with finding the unstable region since complex algebraic equations allow for multiple solutions in the inner part of accretion disc (e.g. Huré 1998 and the references therein). Our attempt to use the vertically averaged disc model also resulted in peculiarities, namely, an inner stable region appeared in addition to the outer stable zone (see Fig. 18).

Therefore we use the code computing the vertical structure of a disc described by Pojmański (1986) (see also Siemiginowska, Czerny & Kostyunin 1996), with new opacities (Różańska et al. 1999). We construct the $log\dot{M}$ vs. $log\Sigma_d$ (i.e. accretion rate versus disc surface density in logarithmic scale) curves for several disc radii since the negative slope of such a curve indicate a thermal instability.

The extension of the radiation pressure instability zone as a function of the accretion rate for the viscosity parameter α in the disc equal 0.03 is shown in Figure 18. This zone is larger than the fraction of the disc covered by the corona according to the model B although it shows the same trend.

The viscosity within a cool disc does not have to be the same as in the hot corona. If we increase the disc viscosity or decrease the coronal viscosity the two regions move closer to each other. For disc viscosity equal 1 the two regions roughly coincide for larger accretion rates but for low accretion rates the instability zone is still slightly larger than the corona covered region.

4 Discussion

Our disc/corona model has significant prediction power. It is only parameterized by the mass of the black hole, the accretion rate and the viscosity parameter α. All measurable quantities, like the ratio of the optically thick disc emission to the hard X-ray emission, the soft and hard X-ray slope and the extension of the spectrum into gamma ray band result from the model, including the trends for the change of these quantities with the accretion rate. The model, therefore, can be tested against the observational data.

Qualitatively, the model shows most of the trends seen in the data correctly. According to the model, the hot plasma (corona) temperature is not uniform but lower close to the black hole ($\sim$ 100 keV) and larger further out ($\sim$ 300 keV). Such a trend coincide nicely with the determination of the temperature structure in Cyg X-1 in a low state (Moskalenko, Collmar & Schönfelder 1998). In the case of AGN the quality of the data is not high enough to model any departure from a single temperature fits to X-ray data but the typical value

determined from the data is consistent with the radially averaged value given by our model.

The radial extension of the hot plasma ($\sim 100 - 1000\ R_{Schw}$ in our model) is also consistent with the size of the outer corona determined by Moskalenko et al. (1998). It is significantly larger than in spectral data fitting models of Cyg X-1 and other GBH (e.g. Poutanen et al. 1997) but it may be even still too compact to satisfy the requirements imposed by the variability analysis of Cyg X-1 (Cui et al. 1997). No similar constraints are available for AGN.

Our model predicts that the decrease of the accretion rate results in a relative increase in the hard X-ray emission. Therefore, it qualitatively reproduces the time evolution of X-ray novae (Czerny, Witt & Życki 1996) although more careful data fitting is required to confirm this conclusion (Janiuk et al., in preparation). In the case of AGN, it reproduces well the mean quasar spectrum and the α_{ox} index for most Seyfert galaxies and quasars although there are a few objects with the Big Blue Bump more profound than expected from the model (Czerny, Witt & Życki 1997). Also the variability of NGC 5548 can be well represented as variations of the accretion rate in our model (Kuraszkiewicz et al. 1997). Our model supports the view that Narrow Line Seyfert 1 (NLS1) galaxies are characterized by higher luminosity to the Eddington luminosity ratio than most Seyfert galaxies (Kuraszkiewicz et al. 1998).

Although the model is quite successful in reproducing the overall spectral trends in accreting black holes some problems remain.

Phenomenological models fitted to AGN and GBH indicate higher optical depth of the corona than the values predicted by the model. The results of Moskalenko et al. (1998) might indicate that this problem is limited to the innermost part of the corona. It may be related to the fact that a number of papers suggest both on the basis of the maximum temperature achieved by the optically thick disc and on the basis of the normalization of the reflection component in X-rays that the disc may not extend down to the marginally stable orbit. It is even more clearly seen on a diagram showing the correlation between the energy index of the 'primary hard X-ray power law' versus the strength of the reflection component from the disc (Zdziarski, Lubiński & Smith 1998). If the optically thick flow is actually disrupted in the innermost part the optical depth of the hot flow might increase. It may be caused by disc evaporation (e.g. Dullemond 1999).

Also the prediction of the change of the coronal size with the accretion rate may not be correct. In our model larger accretion rate results in expansion of the corona and relative shift of the hard X-ray generation outwards. It (correctly) leads to a relative decrease of hard X-ray power but at the same time predicts that the size of the corona increases so we would expect an

increase in any time delays observed in X-rays while the opposite is true, at least in Cyg X-1 (Cui et a. 1997). This problem may be again connected with the possibility of the disruption of the disc in its innermost part since both the power density spectra and time delays in Cyg X-1 indicate two component behavior.

The model is very sensitive to the description of the underlying microscopic processes. Further work is clearly needed and at present it is difficult to tell whether more advanced parameterization (particularly of the disc/corona transition) will improve the model or disqualify it.

Our model is not the only model of accretion onto a black hole. It is based on a number of assumptions which may not be justified, mostly an assumption that the hot phase itself also accretes and the gravitational energy of that phase is converted into kinetic energy of ions which in turn heat electrons through Coulomb interaction. Models based on different assumptions can be formulated, like advection-dominated accretion flow model (e.g. Esin et al. 1997), accretion flow with shocks (e.g. Chakrabarti & Titarchuk 1995, Chakrabarti 1997). Since the classical disc is thermally unstable in the radiation pressure dominated regions a clumpy accretion disc is also a very attractive possibility. Outlines of such models were recently discussed by a number of authors (e.g. Collin-Souffrin et al. 1996, Krolik 1998). However, since all models are based on assumptions difficult to support on purely theoretical grounds the best approach is to formulate all models in a way which allows to compare them with broad band spectral data as well as variability properties.

5 Conclusions

The accreting corona model reproduces qualitatively a number of properties of AGN and GBH spectra, including the value of the typical electron temperature and the trends in the spectral changes with the change of the accretion rate. Also the initial half-qualitative comparison with the data for a number of objects is encouraging (Kuraszkiewicz et al. 1997 for NGC 5548, Czerny et al. 1997 for quasars and Seyfert galaxies).

Further development of the model is also required. The most important task is to improve the description of the condition for the disc/corona transition in the case of two-dimensional flow. Reconsideration of this transition, taking into account both radiative and conductive heat transport, may modify the predicted fraction of energy liberated in the corona as a function of radius. It may also naturally lead to the prediction of disc evaporation: phenomenological model fitting seem to indicate the necessity of such a phenomenon (e.g. Poutanen et al. 1997, Życki, Done & Smith 1998, Loska & Czerny 1997,

Zdziarski et al. 1998).

Acknowledgements

We thank Piotr T. Życki for introducing his Monte Carlo description of the Comptonization process into the coronal code.

References

[1] Begelman M.C., McKee C.F., Shields G.A., 1983, ApJ, 271, 70
[2] Begelman M.C., Chiueh T., 1988, ApJ, 332, 872
[3] Bisnovatyi-Kogan G.S., Lovelace R.V.E., 1997, ApJ, 486, L43
[4] Bisnovatyi-Kogan G.S., Blinnikov S.I., 1977, A&A, 59,111
[5] Björnsson G., Svensson R., 1992, ApJ, 394, 500
[6] Chakrabarti S.K., Titarchuk L., 1995, ApJ, 455, 623
[7] Chakrabarti S.K., 1997, ApJ, 484, 313
[8] Collin-Souffrin S., Czerny B., Dumont A.-M., Życki P.T., 1996, A&A, 314, 393
[9] Cui W., Heindl W.A., Rotschild R.E., Zhang S.N., Jahoda K., Focke W., 1997, ApJ, 474, L57
[10] Czerny B., Czerny M., Grindlay J.E., 1986, ApJ, 311, 241
[11] Czerny B., Elvis M., 1987, ApJ, 321, 305
[12] Czerny B., Witt H.J., Życki P.T., 1997, in *ESA SP-382*, 2nd INTEGRAL Workshop,"The Transparent Universe", eds. C. Winkler, T. Courvoisier and Ph. Durouchoux, p. 397
[13] Czerny B., Witt H.J., Życki P.T., 1996, Acta Astron. 46, 9
[14] Czerny B., Zbyszewska M., 1991, MNRAS, 249, 634
[15] Di Matteo T., Fabian A.C., Rees M.J., Carilli C.L., Tvison C.L., 1998, astro-ph/9807245
[16] Dove J.B., Wilms J., Begelman M.C., 1997, ApJ, 487, 747
[17] Dörrer T., Riffert H., Staubert R., Ruder H., 1996, A&A, 311, 69
[18] Dullemond C.P., Turolla R., 1998, ApJ, 503, 361
[19] Dullemond C.P., 1999, A&A, 341, 936
[20] Esin A.A., McClintock J.E., Narayan R., 1997, ApJ, 489, 865
[21] Frank J., King A.R., Raine D., 1995, Accretion Power in Astrophysics, Second Edition, Cambridge University Press, Cambridge
[22] Gammie C.F., 1998, MNRAS, 297, 929
[23] Gammie C.F., Popham R., 1998, ApJ, 498, 313
[24] Gierliński M., et al., 1997, MNRAS, 288, 958

[25] Gondek D., et al. 1996, MNRAS, 282, 646
[26] Górecki A., Wilczewski W., 1984, Acta Astr., 34, 141
[27] Haardt F., Maraschi L., 1991, ApJ, 380, L51
[28] Haardt F., Maraschi L., Ghisellini G., 1994, ApJ, 432, L95
[29] Huré J.-M., 1998, A&A, 337, 625
[30] Janiuk A. Życki P.T. Czerny B. 1999, MNRAS (submitted)
[31] Johnson W.N., McNaron-Brown K., Kurfess J.D., Zdziarski A.A., Magdziarz P., Gehrels N., 1997, ApJ, 482, 173
[32] Kato S., Nakamura K.E., 1998, PASJ, 50, 559
[33] Kato S., Fukue J., Mineshige S., 1998, Black Hole Accretion Discs, Kyoto University Press, Kyoto
[34] Kazanas D., Hua X.-M., Titarchuk L., 1997, ApJ, 480, 735
[35] Krolik J.H., 1998, ApJ, 498, L13
[36] Krolik J.H., McKee C.F., Tarter C.B., 1981, ApJ, 249, 422
[37] Kuraszkiewicz J., Loska Z., Czerny B., 1997, Acta Astr. 47, 263
[38] Kuraszkiewicz J., Wilkes B.J., Czerny B., Mathur S., 1998, submitted to ApJ
[39] Kurpiewski A., Kuraszkiewicz J., Czerny B., 1997, MNRAS, 285, 725
[40] Liang E.P.T., Price R.H., 1977, ApJ, 218, 247
[41] Ling J.C. et al. 1997, 484, 375
[42] Loska Z., Czerny, B. 1997, MNRAS, 284, 946
[43] Maciołek-Niedźwiecki A., Krolik J.H., Zdziarski A.A., 1997, ApJ, 483, 111
[44] Magdziarz P., Blaes O., Zdziarski A.A., Johnson W.N., Smith D.A., 1998, MNRAS, 301, 179
[45] Moskalenko I.V., Collmar W., Schönfelder V., 1998, ApJ, 502, 428
[46] Narayan R., Kato S., Honma F., 1997, ApJ, 476, 49
[47] Pojmański G., 1986, Acta Astr., 36, 69
[48] Poutanen J., Krolik J.H., Ryde F., 1997, MNRAS, 292, L21
[49] Pozdnyakov L.A., Sobol I.M., Sunyaev R.A., 1983, Ap. Space Phys. Rev., 2, 189
[50] Pringle J.E., Rees M.J., Pacholczyk A.G., 1973, A&A., 29, 179
[51] Pringle J.E., 1976, MNRAS, 177, 65
[52] Quataert E., Narayan R., 1998, in 19th Texas Symposium on Relativistic Astrophysics and Cosmology, eds. J. Paul, T. Montmarle and E. Aubourg
[53] Różańska A., 1999, MNRAS, 308, 751
[54] Różańska A., Czerny B., 1996, Acta Astr., 46, 233
[55] Różańska A., Czerny B., Życki P.T., Pojmański G., 1999, MNRAS, 305, 481
[56] Shakura N.I., Sunyaev R.A., 1973, A&A, 24, 337
[57] Shakura N.I., Sunyaev R.A., 1976, MNRAS, 175, 613
[58] Shapiro S.L., Lightman A.P., Eardley D.M., 1976, ApJ, 204, 187
[59] Siemiginowska A., Czerny B., Kostyunin V., 1996, ApJ, 458, 491
[60] Spitzer L., Jr, 1962, "Physics of fully ionized gases", New York, Wiley

[61] Stepney S., Guilbert P.W., 1983, 204, 1269
[62] Svensson R., Zdziarski A.A., 1994, ApJ, 436, 599
[63] Wandel A., Liang E.P., 1991, ApJ, 380, 84
[64] Witt H.J., Czerny B., Życki P.T., 1997, MNRAS, 286, 848
[65] Zdziarski A.A., 1998, MNRAS, 296, L51
[66] Zdziarski A.A., Lubiński P., Smith D.A., 1999, MNRAS, 303, L11
[67] Życki P.T., Collin-Souffrin S., Czerny B., 1995, MNRAS, 277, 70
[68] Życki P.T., Done C., Smith D.A., 1998, ApJ, 496, L25